Separating Different Scales of Motion in Time Series of Meteorological Variables

Robert E. Eskridge,* Jia Yeong Ku,+ S. Trivikrama Rao,+
P. Steven Porter,# and Igor G. Zurbenko&

ABSTRACT

The removal of synoptic and seasonal signals from time series of meteorological variables leaves datasets amenable to the study of trends, climate change, and the reasons for such trends and changes. In this paper, four techniques for separating different scales of motion are examined and their effectiveness compared. These techniques are PEST, anomalies, wavelet transform, and the Kolmogorov–Zurbenko (KZ) filter. It is shown that PEST and anomalies do not cleanly separate the synoptic and seasonal signals from the data as well as the other two methods. The KZ filter method is shown to have the same level of accuracy as the wavelet transform method. However, the KZ filter method can be applied to datasets with missing observations and is much easier to use than the wavelet transform method.

1. Introduction

Some physical–numerical models predict that the doubling of CO_2 gas in the atmosphere will lead to an increase in tropospheric temperatures and a decrease in stratospheric temperatures. To investigate this hypothesis and describe the climate, the National Climatic Data Center (NCDC) and the All-Union Research Institute of Hydrometeorological Information, Russia, have produced a worldwide upper-air dataset called CARDS (Comprehensive Aerological Reference Data Set) (Eskridge et al. 1995a,b) for the period 1946–94. This dataset has been compiled from 20 datasets (R. Eskridge et al. 1997, manuscript submitted to *Bull. Amer. Meteor. Soc.*) and quality controlled by a complex quality control (CQC) developed for this project (Alduchov and Eskridge 1996).

*National Climatic Data Center, Asheville, North Carolina.
+New York State Department of Environmental Conservation, Albany, New York.
#University of Idaho, Idaho Falls, Idaho.
&State University of New York at Albany, Albany, New York.
Corresponding author address: Dr. Robert E. Eskridge, National Climatic Data Center, 151 Patton Ave., Asheville, NC 28801-5001.
E-mail: beskridg@ncdc.noaa.gov
In final form 26 February 1997.

Radiosonde data contain instrument, systematic, and gross errors. Gross or rough errors arise primarily in the transmission of the data or in later processing of data (Gandin 1988). The CQC program developed at NCDC can detect these gross errors and either correct or modify approximately 50%–75% of them. Systematic errors in time series data are due primarily to changing radiosonde sensors or data reduction procedures. Systematic errors can be detected using station histories, mathematical–statistical methods (Zurbenko et al. 1996; Zhai and Eskridge 1996), and physical models of radiosonde temperature sensors (Luers and Eskridge 1995; Luers 1996). Systematic errors can be minimized (corrected) if station history data are well documented and readily available. Instrument and observation errors tend to be normally distributed with a zero mean; that is, they have no bias. Instrument or observational errors cannot be removed from the data and act as noise. Hence, averaging the data or applying an appropriate filter can minimize these errors.

The presence of various scales of motion in time series can complicate the analysis and interpretation of long-term trends in meteorological variables. In the following, it will be shown that high-frequency (short term) variations composed of meso- and synoptic-scale motions act like noise in time series.

The yearly cycle, which represents the seasonal variation, is not regular and the year to year variation in seasonality is so large that it must be accurately removed in order to perform statistical tests, which require that the data are statistically independent and identically distributed for detecting long-term trends in the data. Following the Rao and Zurbenko (1994) method, it is assumed that the time series of a meteorological variable can be partitioned as

$$X(t) = e(t) + S(t) + W(t) + T(t) + E(t), \qquad (1)$$

where X represents the radiosonde time series data, e represents the long-term signal, S represents the seasonal cycle, W represents the meso- and synoptic-scale variations, T represents turbulence, $E(t)$ is the instrument error, and t is time. In upper-air data, the usual frequency of observations is 12 h. This means that energy due to turbulence will not be correctly resolved and will be falsely represented in lower frequencies (aliasing). The Nyquist frequency for radiosonde data is 24 h. Small mesoscale flow features will not be adequately sampled by the radiosonde network and their energies are also folded into lower frequencies. Hence, the $T(t)$ term can be dropped from (1). Random and systematic errors, represented by $E(t)$, are ignored in this paper.

The model presented in (1) is based on the assumption that there are gaps in the spectra. Synoptic-scale events have a timescale ranging from 2 days to 3 weeks. The next scale is the seasonal with a period of 1 yr, and finally scales longer than a year. Figure 1 shows the 850-mb temperature data from Hong Kong as a raw time series, the separated short term, and seasonal components. The method used to create Figs. 1b and 1c is presented in section 2.

2. Separation of synoptic and seasonal components in time series

The PEST algorithm (Brockwell and Davis 1991) and the monthly anomaly technique (Wilks 1995) are two methods that are commonly used to separate various timescales in time series data. In this paper, it will be shown that these two techniques have shortcomings. The wavelet transform and KZ filter methods are shown to be capable of separating the various timescales with minimal errors.

The Kolmogorov–Zurbenko (KZ) filter (Rao and Zurbenko 1994; Zurbenko et al. 1996) is based on an iterative moving average that removes high-frequency (with respect to the window size) variations from the data. The moving average is computed by

$$y_i = \frac{1}{2q+1}\sum_{j=-q}^{q} x_{i+j}, \qquad (2)$$

where $2q + 1$ is the length of the filter window, y_i becomes the input for the second pass, and so on. By modifying the window length and the number of iterations, the filtering of different scales of motion can be controlled. To filter all periods of less than P days, the following criterion is used:

$$D \times N^{\frac{1}{2}} \le P \qquad (3)$$

where D ($D = 2q + 1$) is the window size in days and N is the number iterations. A more detailed description of how one chooses the parameters P and N is provided by S. Rao et al. (1997, manuscript submitted to *Bull. Amer. Meteor. Soc.*).

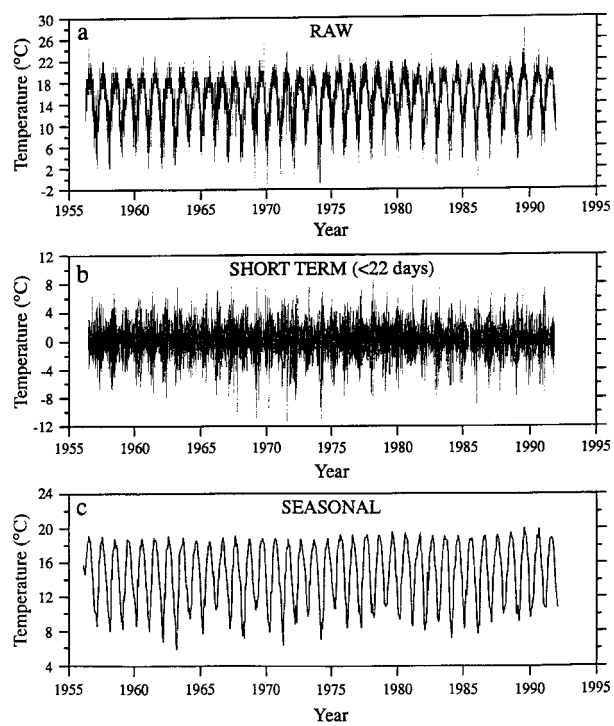

FIG. 1. 850-mb temperature data from Hong Kong: (a) the raw data, (b) the short-term component, and (c) the seasonal component.

Recently, Lau and Weng (1995) applied the wavelet transform technique to climate data. The wavelet transform was shown to be a powerful method for separating different timescales in time series. This paper provides a comparison between the results of wavelet transform and the KZ filter method.

Lau and Weng (1995) describe the wavelet transform as a generalized form of the windowed Fourier transform. A wavelet transform uses local base functions (called wavelets) that can be separately stretched and translated in frequency and time. In this way, the wavelets can be scaled to match the low- and high-frequency signals with the least number of base functions (see Lau and Weng 1995 for details).

PEST (described in detail by Brockwell and Davis 1991) produces a seasonal adjustment that begins with the difference between the raw data and a 1-yr moving average. The difference, which contains seasonality but no long-term trend, is then averaged by season. For example, all January differences (January raw data minus 1-yr moving average value for January) are averaged, producing a seasonal adjustment that is unchanged from year to year. The seasonal adjustment is subtracted from the raw data, leaving behind short-term fluctuations plus long-term trend. A problem with data seasonally adjusted using PEST is the serial correlation in the data introduced by the moving average.

A fourth way of removing both short-term and seasonal variations from time series is to compute perturbations or anomalies (Wilks 1995). An anomaly is the departure of a variable from its long period average value for the given location. This can be accomplished in several ways. First, the averages for each month or season can be calculated for the period of record. Then, the deviation of each data point from the calculated average form a time series. A second method is to calculate a moving average of 30 (90) days simulating a monthly (seasonal) average and calculate the deviations from this average. This second method permits the study of the characteristics of anomalies. Time series of anomalies are approximately stationary.

In the following analysis, high-frequency meso- and synoptic-scale variations are removed by smoothing the data with the KZ filter for a window size of 15 days and 5 iterations. This filter will remove all cycles of less than 33 days. Figure 2 shows the spectra of the unfiltered temperature data from Hong Kong for 850 mb, and Fig. 3 shows the spectra of the data filtered with KZ(15,5). The energy levels in periods less than 33 days have been reduced by factors of 10–100. The lag autocovariance of the Hong Kong temperature data (raw); KZ(15,5) time series, which is identified as KZ seasonal (see Fig. 1c); and the time series created by subtracting the KZ(15,5) series from the original data (short term, see Fig. 1b) are shown in Fig. 4a. The autocovariance is plotted in Fig. 4a because it is additive, whereas the autocorrelation is not. Lag autocorrelation plots are similar to the lag autocovariance plots. Fig. 4a shows that the original data have a nonzero lag autocovariance out to 90 days (seasonality) and the KZ(15,5) time series has a similar lag correlation past 30 days. When the KZ(15,5) series is subtracted from the

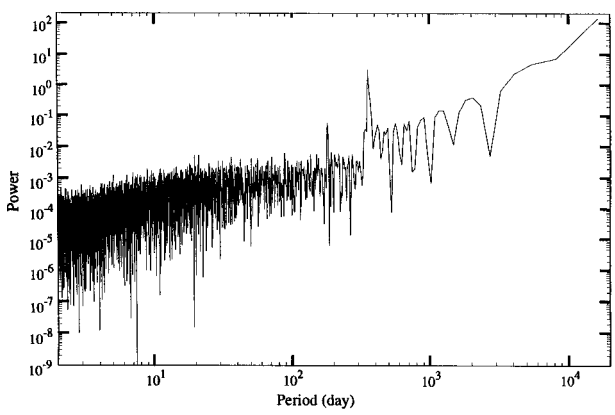

FIG. 2. Power spectra of the 850-mb temperature data from Hong Kong.

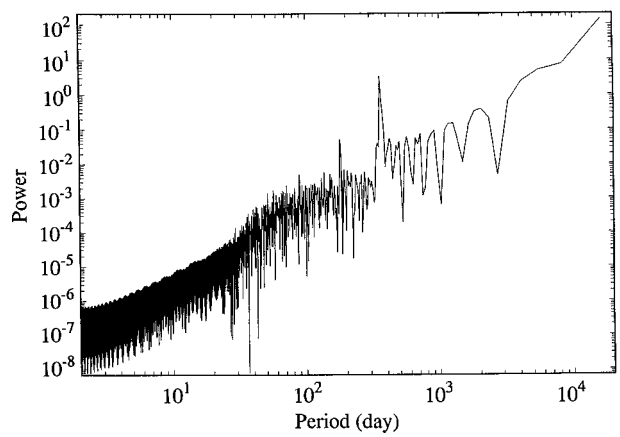

FIG. 3. Power spectra of the 850-mb temperature data after being filtered with KZ(15,5). Frequencies greater than 33 days are left.

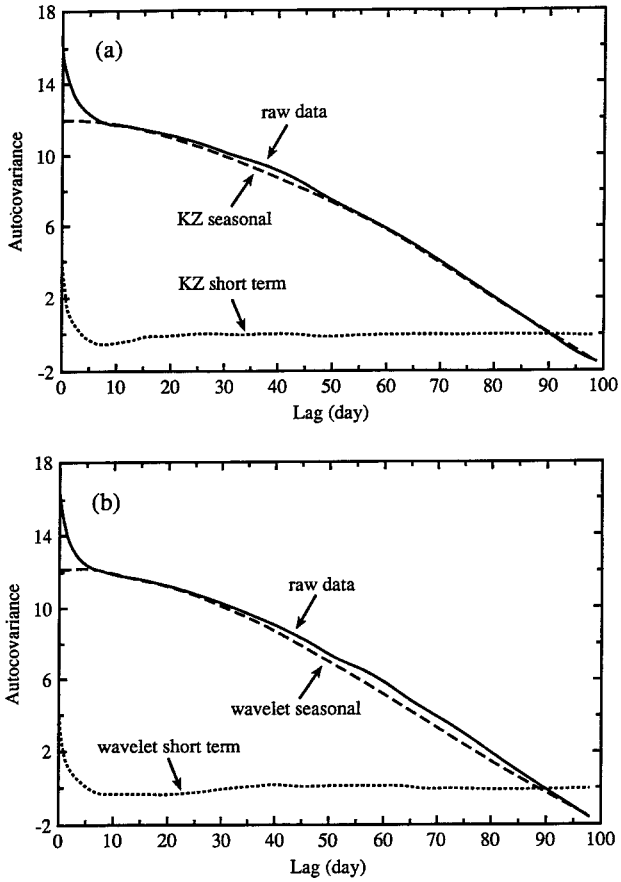

FIG. 4. Lag autocovariance of the time series of the raw data, the short-term component, and the seasonal component.

original time series, it contains only high-frequency data and its lag correlation goes to zero rapidly. Hence, the short period cycles of less than 25 or 30 days resemble random fluctuations (white noise). Meso- and synoptic-scale motions are contained in these frequencies. A lag correlation or covariance of a time series containing just the seasonal component should be sinusoidal in shape, and it is (see Fig. 1c). Figure 4b shows plots of the lag covariance of the raw data, wavelet seasonal, and wavelet short-term component. The curves in Figs. 4a and 4b are very similar.

The yearly cycle and all smaller timescales can be removed by picking a larger window size. The results from the KZ filter with three iterations and a window of 365 days for the temperature data are shown in Fig. 5; the resulting time series contains cycles with periods greater than 1.7 yr. A linear fit to these data will reveal any long-term trend. It should be noted that a trend may be created or affected by instrument changes, changes in data reduction techniques, and actual climatic variation. The change in observation time from 0300 and 1500 UTC to 0000 and 1200 UTC on 1 July 1957 is evident in Fig. 5. In 1957, there is a temperature decrease of 2°C.

To isolate the seasonal signal, the long-term signal and meso- and synoptic-scale variations have been removed from the Hong Kong time series

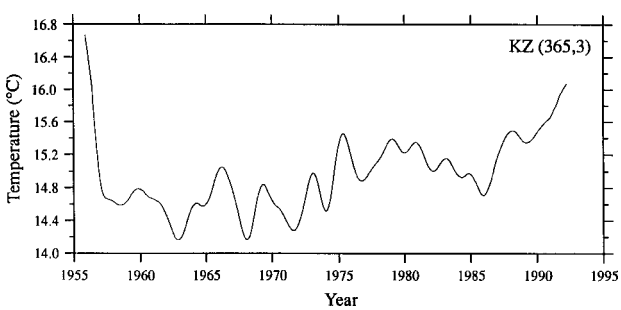

FIG. 5. Time series in which short-term and seasonal frequencies have been removed.

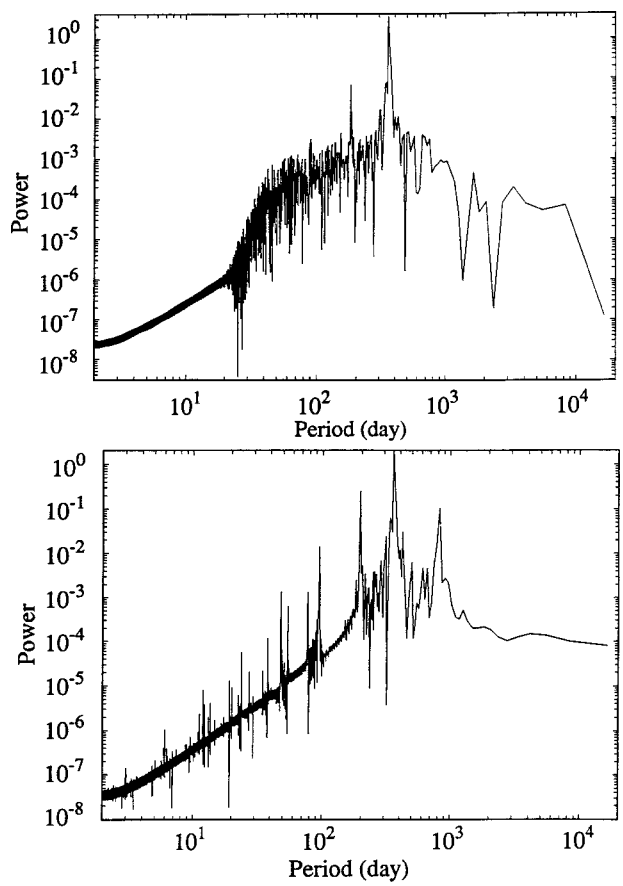

FIG. 6. Power spectrum for the KZ filter method in (a) and the wavelet transform method in (b) after the short-term and seasonal components have been removed.

using the KZ filter method and the wavelet transform method. The power spectrum of filtered temperature time series are shown in Figs. 6a and 6b for the KZ and wavelet transform methods, respectively. The wavelet transform has isolated the seasonal cycle cleanly from the long-term signal, but not the meso- and synoptic scales. The spikes for periods below 100 days (high frequencies) indicate some meso- and synoptic-scale signals are retained. The KZ method has eliminated the meso- and synoptic scales cleanly as can be seen by comparing Fig. 6a to Fig. 2. It has isolated the seasonal signal from the long-term signal. The KZ method appears to be more effective at removing the meso- and synoptic scales from the time series than the wavelet transform. The power spectra for periods greater than 700 days are similar for the wavelet and the KZ filter with the variance being somewhat lower for the KZ method. The separation of long-term phenomena from other parts of the spectrum are important in order for detecting long-term trends. Since further study into filter performance with respect to the separation of low-frequency phenomena from long-term trends is needed, DiRienzo et al. (1997) are examining a promising new technique for detecting small features of power spectrums.

The effectiveness of the KZ and wavelet transform methods in separating different timescales is shown in Figs. 7a and 7b. In these two plots, the seasonal component is plotted against the short-term component after spectral decompositions of time series. The correlation between the short-term and seasonal time series produced by the KZ method is 0.057, and the correlation between the two time series produced by the wavelet transform is −0.0017. When the high-frequency and seasonal components are cleanly separated, the correlation between the time series comprising high-frequency and seasonal components should be near zero, and both are. The scatterplots are very similar, showing that both the seasonal and synoptic scales have been correctly isolated by these two methods.

A simulated anomaly can be created with the KZ filter by subtracting from the original time series a time series created with a window of 30 days and one iteration, KZ(30,1). The spectra of the KZ(30,1) series are shown in Fig. 8. This figure shows that the amplitude of the high-frequency cycles have been reduced for all periods below 30 days. The spectra shows various peaks of energy at periods below 40 days. Figure 9a presents the

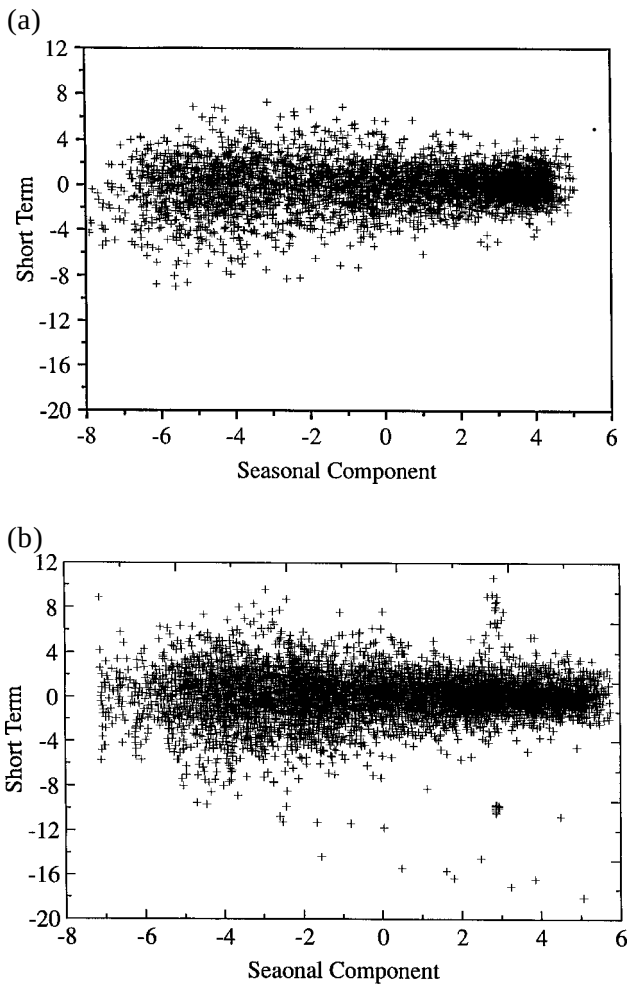

FIG. 7. Plot of the seasonal temperature component against the (a) short-term temperature component for the KZ filter and (b) the wavelet transform method.

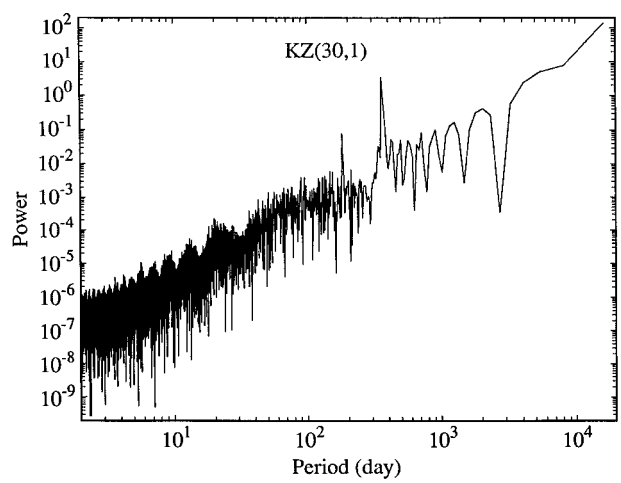

FIG. 8. Power spectra for the time series KZ(30,1) of the simulated anomaly method.

lag autocorrelation for the temperature data, the data filtered by PEST, anomalies, and [original time series data—KZ(15,5)] identified as KZ in the plot. The problem in working with the unfiltered data is clearly shown by the cyclic nature of the lag autocorrelation. The three filtering methods clearly remove part of the seasonal cycle. In Fig. 9b, the scale is expanded to better show the behavior of the lag autocorrelations. Figure 9b shows that data filtered by PEST are cyclic with a 12-month cycle. The autocorrelations for PEST have a maximum of about 0.25 at 24 and 36 months. While anomalies do not show a 12-month pattern like PEST, the time series have a lag autocorrelation of about 0.1, which seems to be increasing with lag. The time series in which the seasonal cycle was removed with the KZ filter is clearly superior to the other two methods; the lag correlation is about 0.025.

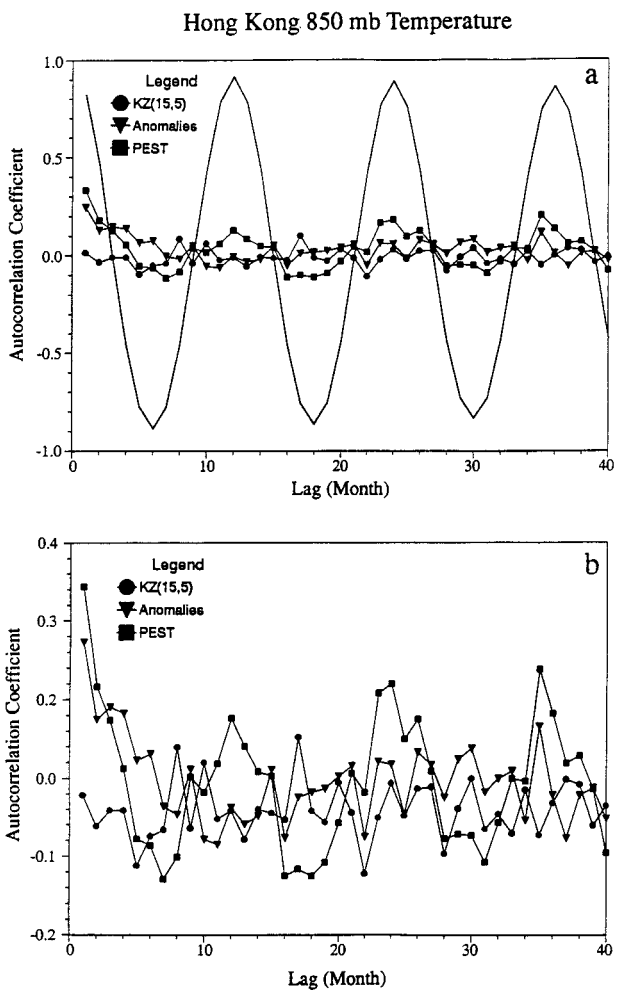

FIG. 9. (a) Lag correlation of raw data, PEST, KZ(15,5), and anomalies. (b) Autocorrelations with an expanded scale.

3. Transfer functions

The behavior of the various filters can be examined by the use of transfer functions (Lumley and Panofsky 1964). A transfer function is defined using the convolution theorem and the definition of spectra by

$$\psi(\omega) = H(\omega)\phi(\omega), \tag{4}$$

where ϕ is the spectral density of the original data, ψ is the spectral density of the filtered data, H is the transform function of the filter, and ω is the frequency. When $H = 1$, the data are passed without modification, and when $H = 0$, the frequency is removed. A perfect filter would be a step function passing frequencies below a specified frequency ω_1 and completely attenuating those above.

The behavior of the KZ filter is shown in Fig. 10. The KZ(30,1) time series shows ringing of the signal, which explains the cyclic behavior found in Fig. 8. This ringing is barely detectable in the KZ(30,2) time series and is essentially zero in KZ(30,3). Figure 10 shows why the meso- and synoptic scales are removed with a KZ(15,5) filter rather than a KZ(33,1) filter. The transfer functions for the KZ(182,3) filter and the KZ(365,3) filter are shown in Fig. 11. Here KZ(365,3) removes frequencies higher than about 1000 days, whereas KZ(182,3) removes frequencies higher than about 500 days.

Figure 12a shows the transfer functions for PEST, KZ(30,1), and KZ(15,5), which all filter out

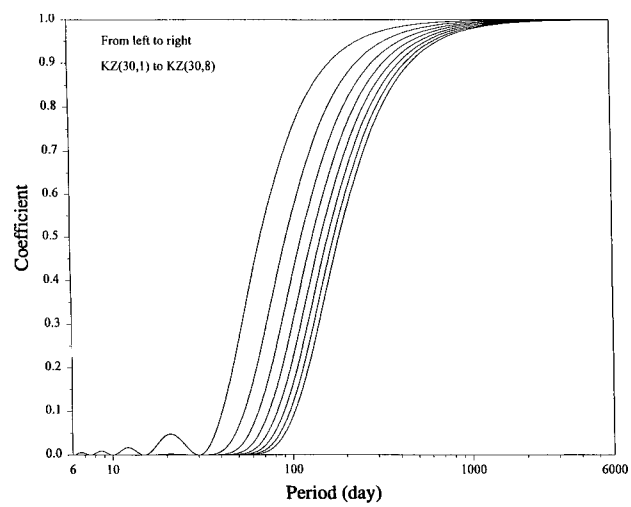

FIG. 10. Transfer function for the KZ filter with a window size of 30 days and the number of iterations varying from one to eight.

the meso- and synoptic scales. The transfer function for the PEST procedure contains a number of spikes, since it deals with monthly averaged data and the transfer function is created based on daily data. The spike in the transfer function near 365 days results in the passing of seasonal signal and explains the 12-month oscillation shown in Fig. 9. The spikes at the higher frequencies mean that some synoptic-scale signals are being passed by the filter.

Monthly anomalies can be defined for a variable $X(t)$ observed for n years in the following way.

1) Apply $KZ_{30,1}$ to $X(t)$, then define $B_{30,1}(t) = KZ_{30,1}\{X(t)\}$;
2) Calculate an average baseline for the n years by $KZ_{30,1}$,

$$AvB_{30,1}(z) = \frac{1}{n}\sum_{k=0}^{n-1} B_{30,1}(z+365k), \qquad (5)$$

also,

$$\begin{aligned} \mathrm{Av}B_{30,1}(t) &= \mathrm{Av}B_{30,1}\left[\mathrm{REM}(t,365)\right] \\ &= \frac{1}{n}\sum_{k=0}^{n-1} B_{30,1}\left[\mathrm{REM}(t,365)+365k\right]. \end{aligned} \qquad (6)$$

The REM function or remainder function is based on the remainder theorem. If a and b are integers and $b > 0$, there exist integers q and r such that $a = qb + r$. Here $a = 365q + r$ and r = *REM* (a,365).

3) Define anomalies $A(t)$ as

$$\begin{aligned} A(t) &= B_{30,1}(t) - \mathrm{Av}B_{30,1}(t) \\ &= (I - \mathrm{Av})B_{30,1}(t)\ . \end{aligned} \qquad (7)$$

The transfer function is calculated as the product of two transfer functions for $KZ_{30,1}$ and $\{I - \mathrm{Av}\}$, where I is the identity function. The first is given by

$$\frac{\sin^2(30\pi\omega)}{30^2\sin^2(\pi\omega)} \qquad (8)$$

and is shown in Fig. 10. The second transfer function is given by

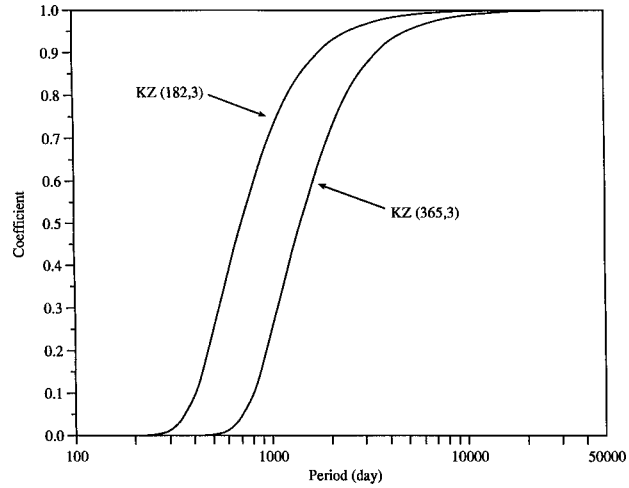

FIG. 11. Transfer function for the KZ filter with window size of 182 and 365 days and three iterations.

$$[1 - h(\omega)]^2, \qquad (9)$$

where $H(\omega) = h^2(\omega)$ is the transfer function given by

$$H(\omega) = \frac{\sin^2(365n\pi\omega)}{n^2\sin^2(365\pi\omega)}, \qquad (10)$$

where ω has units of days per period. The transfer function of anomalies has a very complicated mixture of low and high frequencies and is shown in Fig. 12b.

Traditionally, anomalies $A(t)$ are displayed at the 15th of the month, which keeps the same portion (~5%) of the noise as the procedure above. Noise increases the variability of the output and uncertainty of inferences made with the data. The transfer function shows that anomalies distort frequencies near zero and therefore limit its use in studying long-term trends.

4. Applications of the KZ filter

When the timescale of a problem is known, application of the KZ method is straightforward. For example, to isolate the annual cycle for time series $X(t)$ of hourly, twice daily, or daily meteorological data, calculate a filtered time series using the KZ(15,5), denoted KZ(15,5), which removes periods less than 33 days and the filtered time series

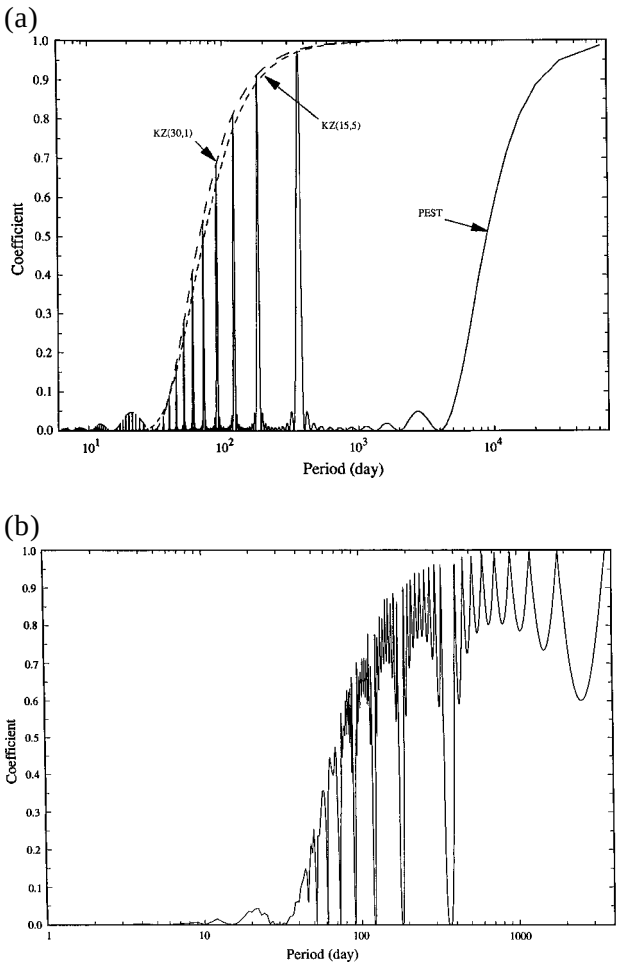

FIG. 12. (a) Transfer function for the PEST method, simulated anomalies (KZ(30,1)), and KZ(15,5). (b) Transfer function for anomalies method.

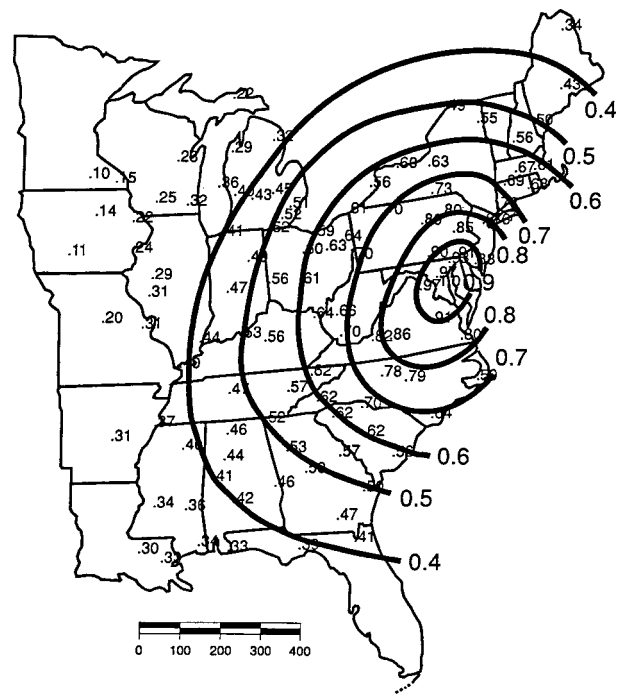

FIG. 13. Isolines of correlations depicting the spatial extent of the synoptic-scale forcing in the surface temperature, extracted by correlating $W(t)$ at Washington, D.C., with $W(t)$ at other stations.

using KZ(720,3), which contains only long-term signals. The time series KZ(15,5) − KZ(720,3) will contain primarily the yearly cycle. When the timescale is not known, it can be determined as demonstrated in the next section.

a. Determination of length and timescales

Eastern U.S. surface temperature data have been used in the following analysis to determine the length and timescale. The various scales of motion embedded in the temperature time series data at each station have been separated using the KZ filter. Once this is accomplished, one has a time series of the variables representing a particular physical forcing element. For example, the information in the synoptic signals $W(t)$ at different locations can be used to characterize the space scale associated with the synoptic forcing. The relationship among $W(t)$ components in temperature data is extracted from the correlation matrix and examined using isolines of correlation (Fig. 13). The space scale for this physical (synoptic scale) forcing is on the order of 1000 km (see Fig. 14), which is the *e*-folding distance for the spatial correlation. One can address the timescale of the $W(t)$ components either by applying a mean wind speed to the spatial scale or by examining the temporal (serial) correlation in $W(t)$. Based on the former, mean wind speeds in the range of 8 to 20 km h^{-1} lead to timescales of 2–5 days. In the case of temporal correlations, since the $W(t)$ resemble a Markov process with 1-day correlations in the range 0.4–0.8, the *e*-folding time ranges from 1 to 4.5 days across the continental United States (S. Rao et al. 1997, manuscript submitted to *Bull. Amer. Meteor. Soc.*). The *e*-folding time in Washington, D.C., temperature data is 1.9 days.

b. Quality control of upper-air data

Near-zero autocorrelations among the values in the high-frequency component (Fig. 4) suggest that the short-term variation in temperature time series could be modeled as white noise. Following Rao

et al. (1996), the temperature time series data can be represented as

$$T(t) = \text{baseline}(t) + N(0, \sigma^2), \qquad (11)$$

where N is noise with a zero mean, standard deviation σ, and

$$\text{baseline}(t) = e(t) + S(t) = \text{KZ}_{15,\,5}. \qquad (12)$$

Equation (12) means that for a given time, t, $T(t)$ is approximately normal with mean baseline(t) and standard deviation σ. For a short time interval, Δt, however, we can only speak about the multivariate distribution of $T(\Delta)$, or its posterior distribution when the baseline is known. Because the baseline changes very slowly, it is easily predictable for a particular day or short time interval for which one may suspect data quality; that is, the baseline can be interpolated for short periods. By imposing white noise on a given baseline (actual or interpolated), the distribution of $T(t)$ or $T(\Delta)$ can be described via simulation and used to construct confidence intervals. To illustrate, Eq. (11) was used to simulate the entire period of record 1000 times. The temperature distribution and associated 95% confidence interval are shown in Fig. 15 along with the observed data distribution. This approach can be followed for a particular day or short interval to supplement the CQC methodology mentioned earlier and improve the quality of radiosonde data.

c. Calculation of trends

The KZ filter, anomalies, and PEST were applied to the Hong Kong temperature data to estimate long-term trends. Confidence intervals were estimated for each filter. The KZ filter was applied with a 730-day window and three iterations to remove all cycles less than 1266 days. Anomalies were calculated by removing the long-term seasonal components from the monthly averaged data. PEST data are calculated by removing the seasonal components from the monthly averaged data (see section 2). Linear regression curves as well as the 95% confidence interval are then calculated by (13) and (14),

$$Y(t) = at + b, \qquad (13)$$

where Y is the filter data and t is time. The width of a 95% confidence interval for a is given by

$$2t_{0.975,\,f}\,\frac{\left[\sum\left(Y-(at+b)\right)^2\right]^{\frac{1}{2}}}{n^{\frac{1}{2}}\left[\sum\left(t-\mu_t\right)^2\right]^{\frac{1}{2}}}, \qquad (14)$$

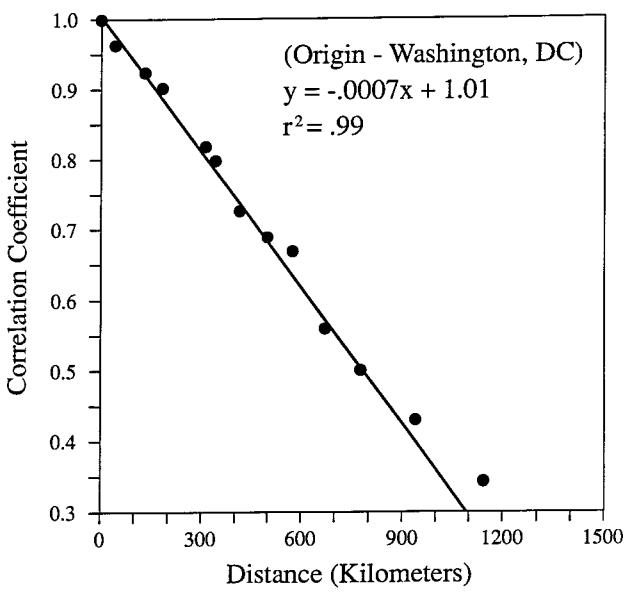

FIG. 14. The decay of correlation among $W(t)$ components as a function of downwind distance from Washington, D.C. The e-folding distance is about 1000 km, representing the spatial scale of synoptic forcing in the surface temperature data.

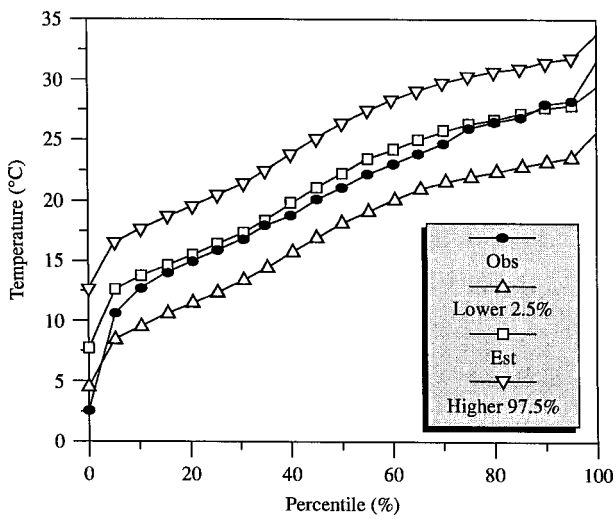

FIG. 15. The cumulative distribution of the simulated temperatures for Hong Kong at 1000 mb along with the 95% confidence interval. Also shown in the diagram is the distribution of the measured values.

where f is the degrees of freedom of the correlated series Y, given by (Loftis and Ward 1979) as

$$f = \frac{n}{1 + \frac{2}{n}\sum_{i=1}^{n-1}(n-i)\rho_i}. \qquad (15)$$

The ρ_i are the autocorrelations at lag time I, and n is the sample size. When n = 10 220 (28 yr of data), and Y is filtered with a KZ(730,3), f = 3.98, and $t_{0.95,3.98}$ = 2.86. Figure 16 shows the data from KZ filter, anomalies, PEST, and the regression lines. Although the magnitude of the long-term trend estimated by the three methods is similar, the KZ filter provides estimates with much higher (about 10 times) confidence than the other methods (see Table 1).

5. Implications and conclusions

The KZ filter can be used to calculate the contribution of various scales of motion to the total variance of the temperature data. For example, analyses of the 850-mb temperature data from Hong Kong show the following.

- The contribution of the short-term component (meso- and synoptic scales) to the total variance is the variance of the [original – KZ(15,5)] time series divided by the total variance. This is about 20% for the Hong Kong temperature data. The total variance is that calculated from the unfiltered temperature data.
- The contribution of the long-term component (trend) to the total variance is the variance of the KZ(365,3) series divided by the total variance. This is about 3% for the Hong Kong temperature data.
- The contribution of the seasonal component to the total variance is the variance of the [raw data—meso- and synoptic scales—long term] time series. This is about 77% for the Hong Kong temperature data.

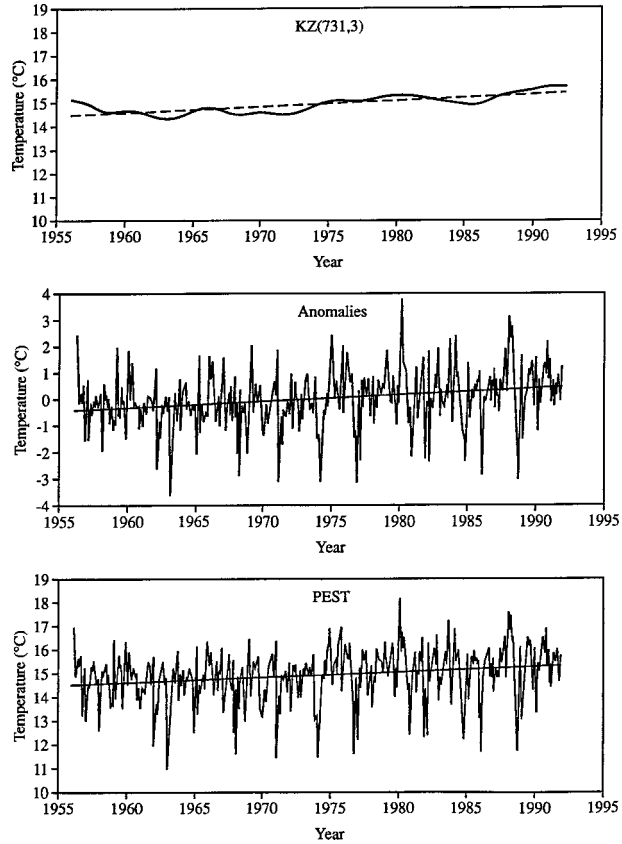

FIG. 16. Filtered time series and the linear trend for (a) KZ method, (b) anomalies, and (c) PEST.

TABLE 1. Values of the long-term trend and confidence intervals for the KZ filter, PEST, and anomalies methods.

	Long-term trend	95% confidence interval
KZ filter	0.024 yr^{-1}	0.00177
Anomalies	0.025 yr^{-1}	0.0260
PEST	0.025 yr^{-1}	0.0270

Clearly, it is essential to cleanly separate the meso- and synoptic scales and seasonal variations from the data to calculate long-term trends correctly. Anomalies and PEST will not adequately remove these frequencies.

The results presented in this paper indicate that the KZ filter method has the same level of accuracy as the wavelet transform method. The KZ filter can be applied directly to datasets containing missing observations because missing values are simply left out of the computation, whereas anomalies, PEST, and wavelet transform methods require that data be created to fill gaps. Also, the KZ filter is very easy to use. Among the four methods ex-

amined here, the KZ filter is the method of choice to detect and track changes in time series of climate variables because of its simplicity and accuracy.

Acknowledgments. CARDS is a joint project of the United States National Climatic Data Center and the All-Russian Research Institute of Hydrometeorological Information. The CARDS program is supported by the U.S. Department of Energy under Contract DE-AI05-90ER61011, the Climate and Global Change program of NOAA, and the National Climatic Data Center.

S. T. Rao and P. S. Porter were supported in part by the National Oceanic and Atmospheric Administration under Contract 50EANE2000078, the U.S. Environmental Protection Agency under Cooperative Agreement R825260-01-0, and the Electric Power Research Institute under Contract WO4447-01. We thank Drs. Harold Crutcher, Nathaniel Guttman, and David Parker for reviewing the paper.

References

Alduchov, O. A., and R. E. Eskridge, 1996: Complex quality control of upper-air variables: Geopotential height, temperature, wind and humidity at mandatory and significant levels. NCDC Rep., 135 pp. [Available from NCDC, 151 Patton Ave., Asheville, NC 28801-5001; NTIS PB97-132286.]

Brockwell, P., and R. Davis, 1991: *Time Series Analysis.* Springer-Verlag, 577 pp.

DiRienzo, A. G., I. G. Zurbenko, and D. O. Carpenter, 1997: Time series analyses of aplysia total motion activity. *Biometrics*, in press.

Eskridge, R. E., O. A. Alduchov, I. V. Chernykh, P. Zhai, A. C. Polansky, and S. R. Doty, 1995a: A Comprehensive Aerological Reference Data Set (CARDS): Rough and systematic errors. *Bull. Amer. Meteor. Soc.*, **76,** 1759–1775.

——, A. C. Polansky, S. R. Doty, and H. V. Frederick, 1995b: A Comprehensive Aerological Reference Dataset (CARDS): The database. NCDC Rep., 45 pp. [Available from NCDC, 151 Patton Ave., Asheville, NC 28801-5001.]

Gandin, L. S., 1988: Complex quality control of meteorological observations. *Mon. Wea. Rev.*, **116,** 1137–1156.

Lau, K. M., and H. Weng, 1995: Climate signal detection using wavelet transform: How to make a time series sing. *Bull. Amer. Meteor. Soc.*, **76,** 2391–2402.

Loftis, J. C., and R. C. Ward, 1979: Regulatory water quality monitoring networks-statistical and economic considerations. U.S. Environmental Protection Agency, EPA-600/4-79-055, 89 pp. [Available from Library Program Service, U.S. Government Printing Office, Washington, DC 20401.]

Luers, J. K., 1996: Temperature correction models for the world's major radiosondes. NCDC Rep., xxx pp. [Available from NCDC, 151 Patton Ave., Asheville, NC 28801-5001; NTIS PB97-132351.]

——, and R. E. Eskridge, 1995: Temperature corrections for the VIZ and Vaisala radiosondes. *J. Appl. Meteor.*, **34,** 1241–1253.

Lumley, J. L., and H. A. Panofsky, 1964: *The Structure of Atmospheric Turbulence.* Interscience Publishers, 239 pp.

Rao, S. T., and I. Zurbenko, 1994: Detecting and tracking changes in ozone air quality. *J. Air Waste Manag. Assoc.*, **44,** 1089–1095.

——, I. G. Zurbenko, P. S. Porter, I. Y. Ku, and R. F. Henry, 1996: Dealing with the ozone non-attainment problem in the Eastern United States. *Environ. Manager*, Jan., 17–31.

Wilks, D. S., 1995: *Statistical Methods in Atmospheric Sciences.* Vol. 59, *International Geophysics Series*, Academic Press, 467 pp.

Zhai, P., and R. E. Eskridge, 1996: Analysis of inhomogeneities in radiosonde temperature and humidity series. *J. Climatol.*, **9,** 884–894.

Zurbenko, I., P. S. Porter, S. T. Rao, J. K. Ku, R. Gui, and R. E. Eskridge, 1996: Detecting discontinuities in time series of upper-air data: Demonstration of an adaptive filter technique. *J. Climatol.*, **9,** 3548–3560.